

3D SIMULATION OF UNDERFILL ENCAPSULATION IN SEMICONDUCTOR PROCESSING

Chih-Chung Hsu², Hsien-Sen Chiu¹, Rong-Yeu Chang²

¹CoreTech System (Moldex3D) Co., Ltd., ChuPei City, Hsinchu, Taiwan

²Department of Chemical Engineering, National Tsing-Hua University, Hsinchu, Taiwan 30043, R.O.C.

ABSTRACT

Semiconductor industry is the leader of industries in Taiwan for more than ten years. The development of microchip product is pretty complicated due to the complexity of material property while processing. Recently it becomes more arduous, because the trend of customer demand is driving the technology of IC packaging toward higher packaging densities with thinner and smaller profiles. Therefore, flip chips have recently gained popularity among manufacturers of many small electronics where the size savings are valuable. Especially, the short wires greatly reduce inductance, allowing higher-speed signals, and also carry heat better. However, fine pitch flip chip molding has difficulty meeting mechanical shock and prevention voids for underfill in on-site process. It becomes the most challenging in industry, so the conventional trial-and-error method is adopted previously to resolve these problems. Yet trial-and-error is difficult and costly because of the complex interactions among fluid flow, heat transfer, structural deformation and polymerization of the underfill.

In this study, a 3D CAE simulation tool is proposed to accurately track the propagation of the underfill in microchips. The proposed methodology developed in this work accounts for most of the physical phenomena believed to play an important role in underfill flows. The results demonstrate not only show how an encapsulant fills an underfill gap, flowing around the bumps, but also simulate the interconnect area between a die and a substrate, and the area surrounding the die. The simulation results shows edge flow effect would help to pull the melt flow front in the bump array and formation of the fillet spread. By using the integrated analysis, molding defects can be easily detected and mold ability problems can be improved efficiently to reduce manufacturing cost and design cycle time.

INTRODUCTION

Recently, for the need of more signal outputs and less heat dissipation, Flip-Chip is the most brilliant encapsulation technology at present. It saves great space and possessed supreme density, which takes advantages of replacing the gold line to joint with base plate as the chip. Underfill is one of the Flip-Chip processes for encapsulation. For the capillary underfill encapsulation, encapsulant is dispensed along the periphery of one or two sides of the chip. Surface tension and heat are the two main mechanical elements that create the capillary action for underfill [1][2].

Under the forces of heat and surface tension, the encapsulant crawls into the desired space underneath the die using capillary action before the encapsulant is cured. This driving force is greatly influenced by the surface tension among encapsulant bumps and substrate, which results in different filling time. While excessive filling time may cause partial curing of the encapsulant before filling finish and lead to substantial manufacturing process delay.

Since the process currently has many challenges in size reduction of Encapsulations, thickness reduction, and the increasing size of semiconductor chips, using the CAE tool to help practitioners to optimize their molding design becomes a necessary tendency. In

this study, we have develop a integrated simulation tools that can model the capillary flow, which is influenced by the surface tension of encapsulant and the contact angle among encapsulant, bumps and substrate of dispensing process for flip chip underfill. It allows users to input real dispensing procedure and predict the underfill front in underfill process.

IMPLEMENTATION DETAILS

Governing Equations:

Theoretically, underfill encapsulation process is a three-dimensional, transient, reactive problem with moving resin front. The non-isothermal resin flow in mold cavity can be mathematically described by the following equations:

$$\frac{\partial p}{\partial t} + \nabla \cdot \rho \mathbf{u} = 0 \quad (1)$$

$$\frac{\partial}{\partial t}(\rho \mathbf{u}) + \nabla \cdot (\rho \mathbf{u} \mathbf{u} - \boldsymbol{\sigma}) = \mathbf{f}_\sigma \quad (2)$$

$$\boldsymbol{\sigma} = -p \mathbf{I} + \eta (\nabla \mathbf{u} + \nabla \mathbf{u}^T) \quad (3)$$

$$\rho C_p \left(\frac{\partial T}{\partial t} + \mathbf{u} \cdot \nabla T \right) = \nabla \cdot (\mathbf{k} \nabla T) + \Phi \quad (4)$$

where \mathbf{u} is the velocity vector, T is the temperature, t is the time, p is the pressure, $\boldsymbol{\sigma}$ is the total stress tensor, \mathbf{f}_σ is the surface force, ρ is the fluid density, \mathbf{k} is the thermal conductivity, C_p is the specific heat, and Φ is the energy source tem.

A volume fraction function f is introduced to track the evolution of the melt front. Where $f = 0$ is defined as the air phase, $f = 1$ as the melt phase and the melt front is located within control volume between 1 and 0. The advancement of f over time is described by the following transport equation:

$$\frac{\partial}{\partial t} f + \nabla \cdot f \mathbf{v} = 0 \quad (5)$$

HRIC (High Resolution Interface Capturing scheme) differencing method [3] is applied to avoid interface being blurred. The surface tension force is described by CSF(Continuum Surface Force) model proposed by Brackbill [4]:

$$\mathbf{f}_\sigma = -\sigma \kappa (\nabla f) \quad (6)$$

Where σ is the coefficient of surface tension and κ is the curvature of free surface.

In this work, the energy source contains two contributions:

$$\Phi = \eta \dot{\gamma} + \dot{\alpha} \Delta H \quad (7)$$

where η is the viscosity, $\dot{\gamma}$ is the magnitude of the rate of deformation tensor, $\dot{\alpha}$ is the conversion rate and ΔH is the exothermic heat of polymerization.

Chemorheology:

The curing reaction of epoxy resins has received much attention using different analyses. In this work, we apply the combined model proposed by Kamal and Ryan [5] to investigate the curing kinetics of the given EMC because of its ability to accurately predict the experimental data. The combined model can be expressed as follows:

$$\frac{d\alpha}{dt} = (k_1 + k_2\alpha^m)(1-\alpha)^n \quad (8)$$

$$k_1 = A_1 \exp\left(-\frac{E_1}{RT}\right) \quad (9)$$

$$k_2 = A_2 \exp\left(-\frac{E_2}{RT}\right) \quad (10)$$

where α is the conversion of reaction, A_1, A_2, E_1, E_2, m, n are model parameters.

During the curing process, the viscosity of epoxy resins changes with temperature and conversion rate. The Castro-Macosko model [6] is adopted to describe the rheological properties of epoxy resins:

$$\eta(\alpha, T) = \eta_0(T) \left(\frac{\alpha_g}{\alpha_g - \alpha} \right)^{C_1 + C_2\alpha} \quad (9)$$

$$\eta_0(T) = A \exp(E_a/RT) \quad (10)$$

where A, E_a, C_1, C_2 are model parameters, α_g denotes gelation conversion at which viscosity curve grows up because of the formation of three-dimensional network structure of the epoxy resins. It should be determined from experiments.

Numerical Method

The collocated cell-centered finite volume method proposed by Chang and Yang [7] is modified to apply in this work. Base on a SIMPLE-like iteration procedure, the method has improved numerical stability and robust convergence. Pressure, velocity, temperature and volume fraction fields are segregated in the solver so that the efficiency can be achieved even for 3D calculation. This model will cooperate with CSF model to catch more accurate surface effect in capillary action.

RESULTS AND DISCUSSIONS

In this section, we first test the accuracy of our simulation tool and demonstrate the effect of contact angle for underfill front shape during the filling stage. While assuming the liquid viscosity, surface tension coefficient and the contact angle are constant, most studies reported in the reference applied the Washburn model to predict the location of the underfill front. We could derive the propagation of the underfill front by filling time to be given:

$$t_{fill,L} = \frac{3\mu}{h\gamma \cos\theta} L^2 \quad (12)$$

where μ is viscosity, h is the gap size, γ is surface tension coefficient, and θ is contact angle. Through the relation of contact angle and filling time as Fig. 1, we would get the trend that the filling time would be less for smaller contact angle. The plot also demonstrates that in the capillary type underfilling process, the propagation velocity of the front decreased continuously as time progressed. So the general use of capillary-type underfill package size would be limited. Too large chip size will make the filling time significantly elongated and no more cost-effective. Furthermore, the results for different contact angle simulation also describe the behavior of surface tension that the underfill front would reach the

equilibrium contact angle during the flowing as Fig. 2. Once the contact angle set as 90 degree, the mathematical value is infinite which makes the filling time unpredictable.

In the second case, we will use a small underfill package as an example to demonstrate that how to apply the developed CAE tool to see the underfill front propagation. The dimension of our package is 1.0 mm wide, 1.0 mm long and 0.05 mm high. The bump pitch is about 0.087 mm and the bump diameter is 0.056 mm. The device layout of bump and geometry is shown in Fig. 5. In this case study, we define two pass as L-shape to move the dispenser. Further, we implement the outlet BC setting to define the surfaces without surface tension that melt would not crawl with this area. The viscosity model and the kinetic model of the test material are shown in Fig. 3& 4. and the used process condition are listed in Table 1.

Under current molding conditions, we can obtain filling analysis results. Fig. 6 shows melt front time results at different filling percentages. From the different stage of filling, we could know the position of moving dispenser and the edge flow effect would help to pull the melt flow front in the bump array and formation of the fillet spread. And the 3D surface tension effect along the thickness direction could be seen among underfill, bumps and substrate of dispensing process for flip chip underfill. Since in the actual capillary filling process, the underfill tends to go around the chip corner and flow along the edge, which is called the edge flow[9]. This kind of phenomena could also be observed in the simulation as Fig. 7. The detour flow would blend out the cavity and can be attributed to that more dispensing amount for the capillary flow.

CONCLUSION

This study proposes a full 3D numerical approach to model the polymer melt filling behaviors in underfill encapsulation process. The effect of capillary action, viscosity and surface tension on the flow behavior in the capillary underfilling process are discussed. Examples simulated by 3-D application have been shown. By using the integrated analysis, molding defects can be easily detected and moldability problems can be improved efficiently to reduce manufacturing cost and design cycle time. In the future work, the numerical results would be confirmed by comparing with more available experimental data to close to the real process.

REFERENCES

- [1] Hui Wang, Huamin Zhou, Yun Zhang, Dequn Li, Kai XuL., *Computers & Fluids*, 44:187-201, 2011.
- [2] Banijamali, B., Mohammed I., Savalia P., "Reliability of fine-pitch flip-chip packages", *Electronic Components and Technology Conference, ECTC 2009*. 59th, 2009.
- [3] Muzaferija S., Peric M., Sames P., Schelin T., "A two-fluid Navier-Stokes solver to simulate water entry", *Proc. Twenty-Second Symposium on Naval Hydrodynamics*, 1998.
- [4] J.U. Brackbill, D.B. Kothe, and C. Zemach, "A Continuum Method for Modeling Surface Tension", *Journal of Computational Physics*, vol. 100, p. 335, 1991.
- [5] M.R. Kamal and M.R. Ryan, *Injection and Compression Molding Fundamentals*, A.I.Isayev (Ed.), Marcel Dekker, Ch. 4, 1987.
- [6] M.R.Kamal, S.Sourour, and M.Ryan, "Integrated Thermo-Rheological Analysis of the Cure of Thermosets", *SPE Tech. Paper*, 19, 187, 1973.
- [7] W. H. Yang and R. Y. Chang, "Numerical Simulation of Mold Fill in Injection Molding Using A Three-Dimensional Finite Volume Approach", *International Journal for Numerical Methods in Fluids*, vol. 37, p. 125, 2001.

- [8] Yang H., Bayyuk, S., Krishnan A., Przekwas A., Nguyen L., Fine P., "Computational simulation of underfill encapsulation of flip-chip ICs. I. Flow modeling and surface-tension effects", Electronic Components & Technology Conference, 48th IEEE, 1998.
- [9] Shih M. F., Young W. B., "Experimental study of filling behaviors in the underfill encapsulation of a flip-chip", Microelectronics Reliability, vol. 49 1555-1562, 2009.

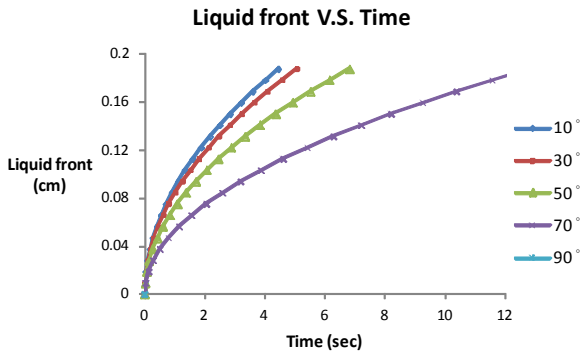


FIGURE 1. Underfill front propagation in a channel due to different contact angle

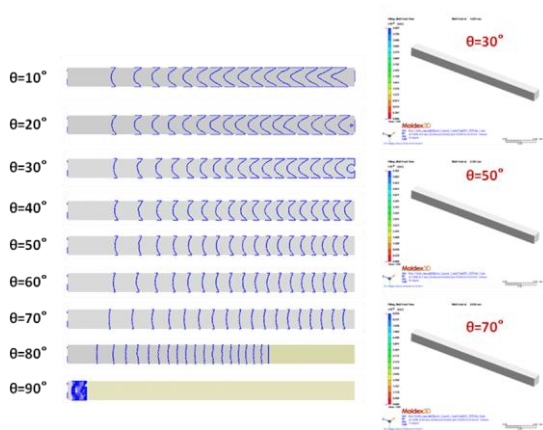


FIGURE 2. Shape revolutions of different contact angle

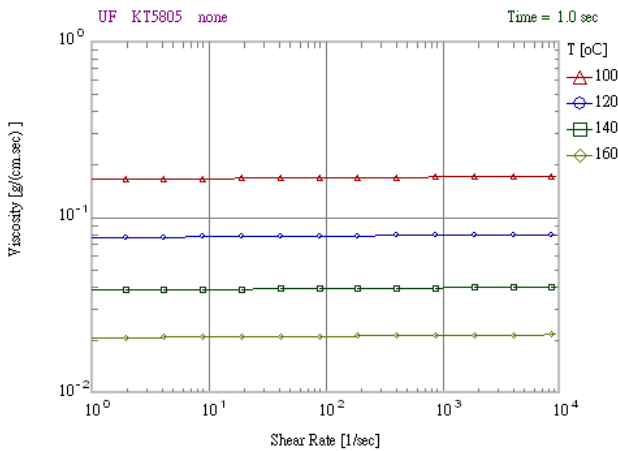


FIGURE 3. Material properties of viscosity

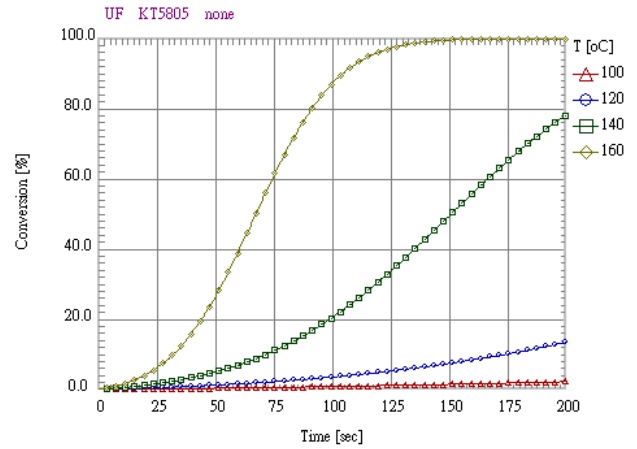


FIGURE 4. Material properties of curing kinetics

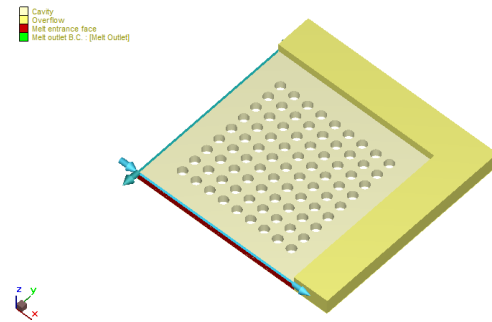


FIGURE 5. Dispenser configuration for a multi-bump underfill flow

Project Settings		Underfill Setting		Cooling Settings	
Condition Setting					
Resin temperature :	100	oC			
Mold temperature :	160	oC			
Cure time :	5	sec			
Dispensing Patterns Setting					
<input type="radio"/> Melt entrance as dispensed pass					
Max. filling time : [] sec					
<input checked="" type="radio"/> Dispensed pass setting Pass Setting...					
Item	Time (sec)	Velocity (mm/sec)			
Maximum filling time	0.1	--			
Pass1	0	1000			
Pass2	0.001	1000			
Surface Tension Properties					
Coefficient :	0.03	N/m			
Contact angle :	30	degree			
Advanced Setting...					

Table 1. Process Condition

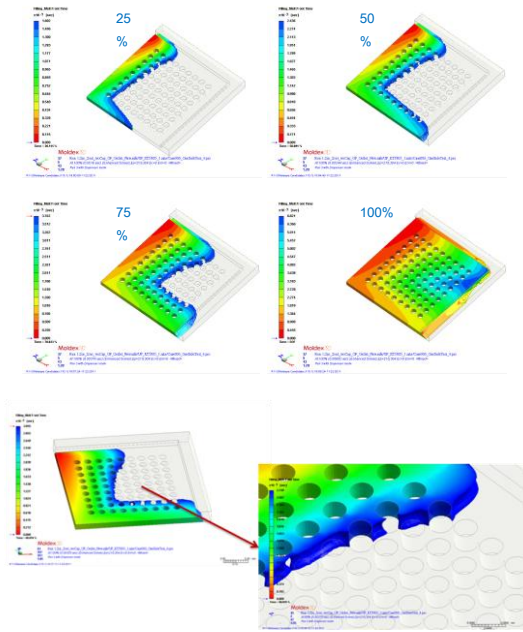


FIGURE 6. Front propagation for a testing underfill problem

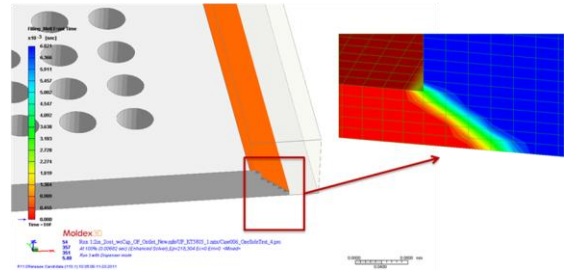
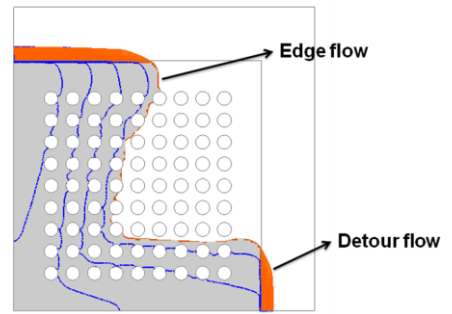


FIGURE 7 Edge and detour flow